Toxicology in Vitro 58 (2019) 170–177

Contents lists available at ScienceDirect

Toxicology in Vitro

journal homepage: www.elsevier.com/locate/toxinvit

Toxicity assessment of wearable wound sensor constituents on keratinocytes

Pulak Bhushan[a], Yogeswaran Umasankar[b], Joshua D. Hutcheson[c], Shekhar Bhansali[a,*]

[a] Department of Electrical and Computer Engineering, Florida International University, Miami, FL 33174, United States
[b] Biomolecular Sciences Institute, Florida International University, Miami, FL 33199, United States
[c] Department of Biomedical Engineering, Florida International University, Miami, FL 33174, United States

ARTICLE INFO

Keywords:
Cytotoxicity
Human keratinocytes
Wearable wound sensor
Cell viability
Mitochondrial activity
Apoptosis

ABSTRACT

This research reports on the cytotoxicity of materials present in a wound biosensor on human keratinocytes (HaCaT) to evaluate the biocompatibility of the sensor for continuous wound monitoring applications. Individual and collective effects of the sensor materials, gold (Au) and silver (Ag) nanoparticles (NPs), uricase enzyme (UOx), ferrocene carboxylic acid (FCA), multi-walled carbon nanotubes (MWCNTs) and poly vinyl alcohol-based polymer (PVA-SbQ) on HaCaT were studied. The toxicology profiles of these materials were derived from cell viability, mitochondrial activity retention and apoptotic behavior studies. At the concentrations present in the sensor, the cell viability studies showed minimal toxicity for Au and Ag NPs, UOx and FCA (cell viability > 75%), while MWCNTs and PVA-SbQ exhibited excellent biocompatibility towards keratinocytes (cell viability > 90%). Resazurin assay confirmed minimal impairment of mitochondrial activity at lower concentrations for all the materials (mitochondrial activity > 0.7). The caspase-3/7 apoptotic assay showed no pronounced apoptotic behavior caused by the materials. The material mixtures studied were Au/UOx/FCA/PVA-SbQ, Ag/UOx/FCA/PVA-SbQ, and MWCNTs/UOx/FCA/PVA-SbQ. A higher toxicity profile was observed for the heterogeneous material mixtures as a result of the cumulative effect of the individual materials. However, the biosensor itself was seen to exhibit lower toxicity (~5%) compared to the material mixtures, due to the protective PVA-SbQ capping over the biosensor. This work establishes the biocompatibility of the reported wound sensor for human measurements with minimal toxic effects on human keratinocytes.

1. Introduction

In an emerging age of wearable medical devices, health risk from exposure to the active materials from these devices is becoming a topic of concern. Wearable sensors that monitor biological activity, disease and metabolism, increasingly integrate biochemical sensors in the sensor suite that interfaces directly with the human body. The wound monitoring sensing systems incorporate physical and biochemical sensors that are in direct contact with tissue and wound fluids. An open wound exposes the underlying human tissue, potentially subjecting it directly to the materials integrated within the sensor. Keratinocytes, a major cellular component of epidermis, play a critical role in the wound healing process. Thus, any material that is toxic to keratinocytes may lead to impaired wound healing. Hence, toxicological screening of the active materials used in these wound sensors need to undergo rigorous testing to determine their biocompatibility. A comprehensive understanding of the cytotoxic effects and the ability of the cells to tolerate active materials is essential for building biocompatible sensing devices.

In vitro human cell culture has emerged as an excellent tool for preliminary toxicity studies. Keratinocytes can be cultured in a physiological fashion and subjected to cytotoxicity tests after being exposed to the active materials of the sensor. Among the three different cytotoxicity tests, extract, direct and indirect contact tests, direct contact is the most sensitive method which yields the most accurate toxicity profiles affecting cell growth, reproduction or morphological effects of a particular cell line. For example, cell viability is observed by assessing cell wall damage. Fluorescent molecules attach to the nucleic acids of membrane compromised cells and fluoresce to indicate the dead cells. The fluorescent microscopy of these tagged cells helps visualize the morphological changes undergone by them. The cellular metabolic activity is measured through assays such as resazurin and MTT (3-(4, 5-dimethylthiazolyl-2)-2, 5-diphenyltetrazolium bromide) assay. Resazurin reduces within the mitochondria proportional to the aerobic respiration inside the cell, providing an insight into the metabolic activity. Toxicity is also probed by examining if the cells undergo apoptosis or necrosis. Apoptosis can be observed by the caspase-3/7 apoptotic assay, wherein the caspases are activated on exposure to the material, leading to cell death. The above tests have been widely

* Corresponding author.
E-mail address: sbhansa@fiu.edu (S. Bhansali).

https://doi.org/10.1016/j.tiv.2019.03.034
Received 11 December 2018; Received in revised form 25 March 2019; Accepted 26 March 2019
Available online 27 March 2019
0887-2333/ Published by Elsevier Ltd.

utilized to determine the toxicity of various materials at both a cellular and intracellular organelle level.

Biochemical sensors are comprised of a combination of materials that sense the target analytes. These materials can be classified into three categories: active sensing materials or reaction catalysts, electron mediators, binders and crosslinkers. Screening of one such active sensing material, Ag ions, suggested that they are toxic to both keratinocytes and fibroblasts (Galandáková et al., 2016; Poon and Burd, 2004). Studies have revealed that both the morphology and the coating on Ag NPs influence their cytotoxic behavior (Bastos et al., 2016; Holmes et al., 2016). Exposure to certain NPs also led to morphological changes in the cellular structure by altering the shape of the cells to fusiform (Arora et al., 2008; Schaeublin et al., 2011; Shvedova et al., 2003). The electron mediators, such as chemically modified carbon nanotubes, were seen to exhibit a dose-dependent decrease in cell viability when treated for 24 h (Monteiro-Riviere et al., 2005). A study also showed that cell morphology changed on altering the surface area and the surface chemistry of the carbon nanotubes (Tian et al., 2006). The binder material, poly-vinyl alcohol (PVA), a commonly used polymer in sensing, has been found to be non-toxic. PVA/PVA-gelatin nanofibers were fabricated in two orientations, and fibroblasts successfully formed confluent layers on them (Huang et al., 2016). A similar result was reported, where excellent cytocompatibility and cell viability was exhibited by nanohydroxyapatite–gelatin–PVA scaffolds (Swain and Sarkar, 2014).

Studies have further shown that some of these materials not only affect the cell viability but also lead to damage of subcellular organelles, like mitochondria and lysosomes. The damage of these subcellular organelles leads to increased levels of reactive oxygen species. For example, cellular uptake of silica (SiO_2) (Kyung et al., 2009), iron (Fe) (Grudzinski et al., 2013) NPs and multi-walled carbon nanotubes (MWCNTs) (Ding et al., 2005) led to mitochondrial disruption. Studies have also shown that a high concentration of NPs decreases the cellular ATP content, leading to a damaged mitochondria (Burd et al., 2007). A study showed that the surface charge on Au NPs regulated their apoptotic inducing nature, wherein a charged Au NP expressed a higher number of apoptotic cells compared to an uncharged NP (Schaeublin et al., 2011). Similarly, Ag NPs at low concentrations were seen to induce negligible apoptotic activity in keratinocytes (Carrola et al., 2016). A number of studies have shown that several other NPs such as TiO_2 and CuO lead to increase in caspase-3 activity, inducing apoptosis (Alarifi et al., 2013; Shukla et al., 2011).

Most toxicity studies aim at understanding the toxicity of each material individually on a desired cell line. Taken together, the interaction between the different materials may manifest unknown toxicological effects. Therefore, understanding and assessment of the collective toxic effects of these materials is critical. In this work, a wound monitoring enzymatic electrochemical sensor was investigated for its potential toxicity on human keratinocytes. The wound sensor constructed by our team had a combination of nanomaterials, active sensing materials and a polymeric binder (RoyChoudhury et al., 2017; RoyChoudhury et al., 2018). The potential toxicity of each individual material was assessed first, following which the collective toxicity of the different combinations of the materials was further examined. This was achieved by incubating the materials/combinations with a human keratinocyte cell line (HaCaT) and then conducting in vitro cell studies. The time and concentration-dependent changes in the cell viability, mitochondrial activity, and apoptotic activity of the cells were then quantified.

2. Materials and methods

2.1. Materials and cells

The Au and Ag NP colloids (10 nm diameter) and MWCNTs (9.5 nm × 1.5 μm) were purchased from Sigma Aldrich, USA. The lyophilized UOx powder, Dulbecco's Phosphate Buffered Saline (DPBS) and glutaraldehyde aq. solution were purchased from Sigma Aldrich and ThermoFisher Scientific, USA respectively. The electron transfer mediator FCA was purchased from Chem-Impex International, Inc. The poly (vinyl alcohol) *N*-methyl-4(4′-formylstyryl)-pyridinium-methosulfate-acetal (PVA-SbQ) was purchased from Polysciences, Inc. The SbQ represents the styrylpyridinium groups attached to the PVA polymer chains. Sodium hydroxide, hydrogen peroxide, sodium phosphate monobasic (NaH_2PO_4) and sodium phosphate dibasic (Na_2HPO_4) used were all of analytical grade. All aqueous solutions were prepared in phosphate buffered saline (PBS) prepared using NaH_2PO_4 and Na_2HPO_4 salts. alamarBlue, cell viability reagent was obtained from ThermoFisher Scientific, USA. Cell culture media, antibiotics and other cell culture reagents were purchased from ATCC. The human epidermal keratinocyte cell line (HaCaT) was kindly provided by Dr. Marcus Cooke at the FIU Department of Environmental Health Sciences, Miami, Florida and was maintained in Dulbecco's Modified Eagle's Medium (DMEM, ATCC) and supplemented with a 10% fetal bovine serum (FBS, ATCC) and 1% antibiotics (penicillin/streptomycin, ATCC). All cells were maintained in an atmosphere of 5% CO_2 at 37 °C.

2.2. Apparatus

UV–vis absorption spectrophotometry of the NP solutions was carried out using an Evolution 300 spectrophotometer (Thermo Scientific). Fluorescence microscopy of the cells was done using a fluorescent microscope (Axio Scope.A1, Zeiss). The fluorescence intensity measurement was performed using a Synergy HTX Multi-Mode microplate reader (BioTek Instruments, USA). A Multiskan™ FC microplate reader (ThermoFisher Sc., USA) was used for absorbance measurements. All cells were maintained in the required atmosphere in a cell culture incubator (Heracell Vios 160i, Thermo Sc.).

2.3. Methods

2.3.1. Material treatment of cells

The NP concentrations for the cell treatments were in the range of 0.5–50 μg ml^{-1} for Au NPs, 0.2–10 μg ml^{-1} for Ag NPs and 0.001–0.1 μg ml^{-1} for the multi-walled CNTs. Similarly, the concentration ranges investigated for the two chemicals, the UOx enzyme and FCA were 0.0005–0.05 U ml^{-1} and 0.2–20 mM, respectively. The prepared PVA-SbQ scaffolds (Supplementary Note S1) of different compositions (5, 8 and 10 wt%) were placed at the bottom of the 96-well plate and the cells were grown on them. The NP concentrations used in the wound sensor were 5 μg ml^{-1}, 2 μg ml^{-1}, and 0.1 μg ml^{-1} for Au, Ag and MWCNTs respectively. Similarly, a concentration of 0.05 U ml^{-1} for UOx enzyme, 2 mM for FCA and 5 wt% for PVA-SbQ was used in the developed sensor.

To assess the collective toxicity, three separate mixtures were prepared, wherein one of the three NPs (Au, Ag and MWCNTs) was added to a mixture of FCA and UOx (1:1) in a 1:1 ratio, resulting in three types of mixtures. Each mixture had three different concentrations prepared such that the involved NPs had varying concentrations, as used in individual studies. The concentrations of UOx (0.05 U ml^{-1}), FCA (2 mM) and PVA-SbQ (5 wt%) were kept constant as used in the sensor. Hereon, the mixture containing Au NPs is denoted as Au_m, and similarly Ag_m and $MWCNT_m$ are the mixtures of Ag NPs and MWCNTs, respectively. Three different biosensors were fabricated using screen-printed carbon electrodes (CHI, Inc., United States). The biosensors were prepared by drop-casting either Au NPs, Ag NPs or MWCNTs, followed by immobilization of UOx and a coating of PVA-SbQ. The biosensor containing Au NPs, Ag NPs or MWCNTs is hereon represented as Au_b, Ag_b and $MWCNT_b$ respectively. Cells were first seeded in a 96 well tissue culture plate (5000 cells/well) and cultured until the desired confluency was reached. Subsequently, the cells were washed with PBS and the growth media was replaced with growth media containing the

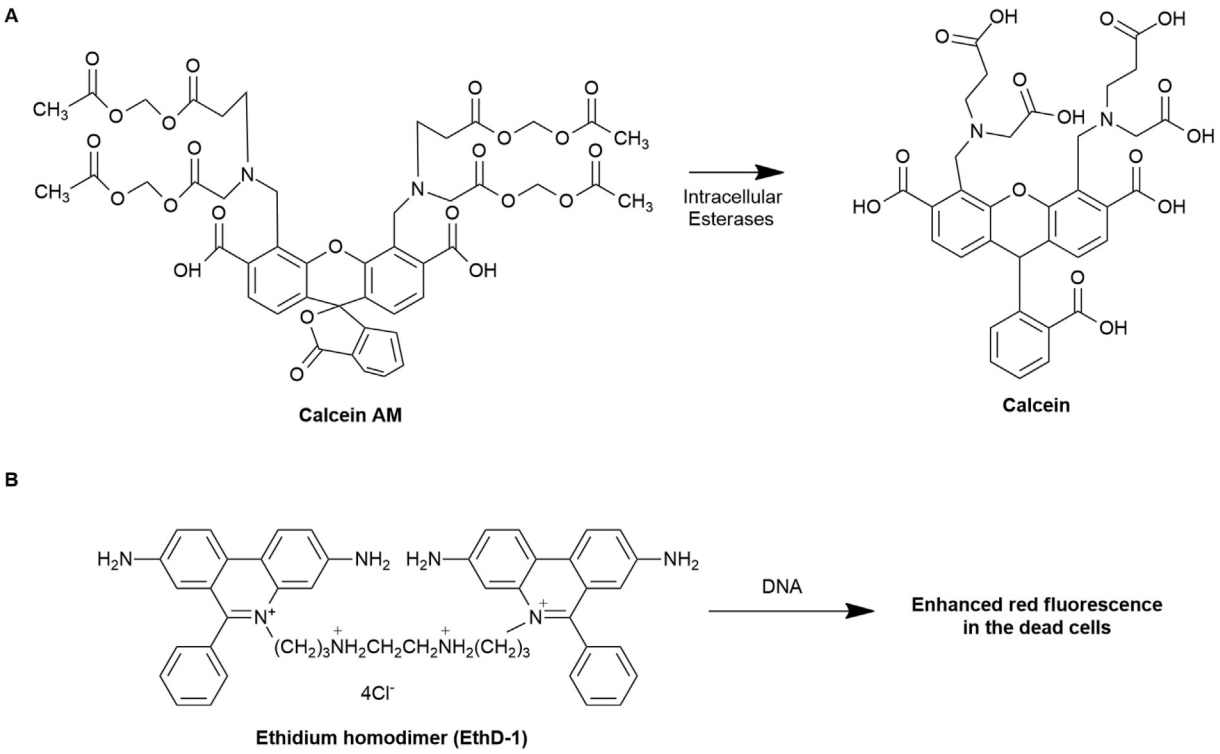

Fig. 1. Chemical reactions involved in determining the plasma membrane integrity and cellular esterase activity of the cell. (A) calcien AM and (B) ethidium homodimer.

chemical, NP or the mixture or the biosensor. The cells were subjected to treatment for 1 h, 2 h, 6 h and 24 h respectively. Growth media without materials served as the negative control for the experiments. After treatment, the cells were washed thrice with PBS before the addition of assay reagents.

2.3.2. Evaluation of cell viability and cellular morphology

The cell viability of keratinocytes treated with the sensor materials was probed in regards to its plasma membrane integrity and cellular esterase activity. Calcein AM and ethidium homodimer were the two dye molecules used to indicate plasma membrane integrity and cellular activity, respectively. In live cells, calcein AM diffuses within the cytoplasm via the plasma membrane and hydrolyzes to produce green fluorescent calcein. This reaction is the result of esterase activity of cells trapped within the cytosol (Fig. 1A). If the cell is dead, ethidium homodimer a membrane impermeant dye molecule intercalates to the free nucleic acids indicating a compromised cell membrane integrity by exhibiting a red fluorescence (Fig. 1B).

To assess the cell viability, a live/dead viability/cytotoxicity kit (ThermoFisher Sc., USA), was used according to the manufacturer's instructions. After treatment, the cells in the 96-well plate were incubated with the dyes at optimal concentrations for 30 min in dark at room temperature. The cells were immediately imaged under a fluorescent microscope. Then, fluorescence intensities were measured using a fluorescence microplate reader. Excitation/emission wavelengths used for calcein AM and ethidium homodimer reagents were 485/528 nm and 528/645 nm, respectively.

2.3.3. Evaluation of mitochondrial activity

The metabolic cell activity of the exposed cells was characterized using the resazurin Alamar Blue assay. The oxidation of resazurin by cellular dehydrogenases inside the mitochondria is reflective of mitochondrial function capacity of the cell. Resazurin undergoes a colorimetric change, pink to red, to form resorufin in response to cellular metabolic reduction, and the fluorescence intensity directly correlates to the number of respiring, living cells (Eq. 1). This is typically attributed to the reduction of resazurin by different oxidoreductase enzyme systems that use NADH/NADPH as the primary electron donor.

$$resazurin_{ox} + 2H^{+} + 2e^{-} \leftrightarrow resazurin_{red} \quad (1)$$

Alamar Blue was added (10% final volume) to the treated cells, which were then incubated at 37 °C. Following an incubation time of 3 h, the absorbance levels were measured using a microplate reader at 570 nm excitation and 620 nm reference wavelengths. A subtraction analysis of the dual wavelength was performed to obtain accurate measurements.

2.3.4. Evaluation of cellular apoptosis

Caspase-3 and caspase-7 are major indicators of apoptosis; these caspases are activated following the leakage of cytochrome C from the mitochondria. The caspase-3/7 assay is a fluorogenic substrate, consisting of a four amino acid peptide (DEVD) conjugated to a DNA binding dye. On activation of caspase-3/7 in the apoptotic cell, the DEVD peptide is cleaved and the dye binds to DNA, producing a bright fluorescence response (Fig. 2). The keratinocytes were incubated with respective materials and mixtures and their apoptotic activity was then measured.

Cell apoptosis was examined using the Caspase-3/7 Green detection reagent (ThermoFisher Sc., USA). 100 µl of the reagent solution was added to each well after a 24 h treatment with the materials. Following this, the cells were incubated at 37 °C for 30 min and fluorescence was measured at excitation/emission wavelengths of 502/530 nm.

2.3.5. Statistical analysis

All data represents the mean ± standard deviation (SD) of three independent culture experiments, with three replicates in each assay.

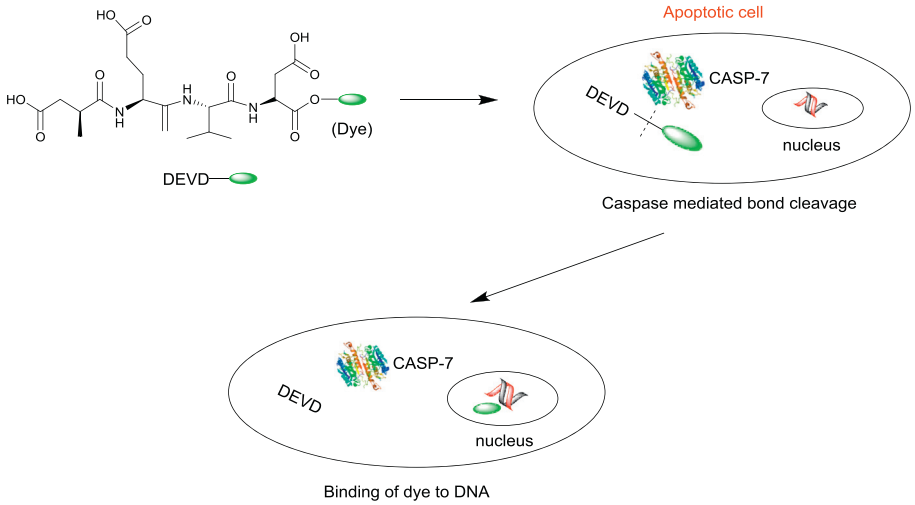

Fig. 2. Schematic illustration of Caspase-3/7 mediated apoptosis detection mechanism.

3. Results and discussion

3.1. Evaluation of keratinocytes viability and cellular morphology

The wound monitoring sensor targeted in this study includes Au NPs, Ag NPs, or MWCNTs as electron transport substrates, UOx as an active catalyst material, PVA-SbQ for enzyme entrapment, and FCA as a mediator. The cell viability studies of these materials showed that the plasma membrane integrity of the treated keratinocytes was compromised, compared to the control cells (Fig. 3A). The treatment with PVA-SbQ showed no toxic behavior, validating that the cells grew and proliferated well on the different PVA-SbQ scaffolds (Fig. 3D). The nanomaterials (i.e. Au NPs, Ag NPs and MWCNTs) and the enzyme UOx also exhibited negligible toxicity on exposure for up to 2 h. However, increasing the cell exposure time to Au, Ag NPs, and UOx resulted in diminished viability (< 85%), but the MWCNTs maintained their non-toxic nature. A concentration-dependent decrease of cell viability was discerned for both Au and Ag NPs, where an exposure for 24 h diminished the cell viability (< 75%) at elevated exposure concentrations (Fig. 3D). Both Au and Ag NPs used in this study have a size of 10 nm, as confirmed by UV–vis spectroscopy (Supplementary Fig. S1). Studies have shown that smaller nanoparticles (≤10 nm) are easily internalized by the cell resulting in a higher cytotoxic nature (Shang et al., 2014). The highly toxic nature of the nanoparticles at higher concentrations may also result from the surfactants used for stabilizing NPs in suspension (Goodman et al., 2004).

The toxic profile of UOx enzyme (Fig. 3A) can be attributed to the hydrogen peroxide (H_2O_2) produced by the enzymatic reaction in the presence of uric acid from the bovine serum added to the growth media. It is well known that higher the concentration of H_2O_2, the lower the cell viability (Thang et al., 2001). Data showed a reduced cell viability at higher UOx concentrations as a result of increased H_2O_2 production (Fig. 3D). An enzymatic assay can be implemented in the future to quantify the amount of H_2O_2 production in the process. On the other hand, the redox mediator FCA induced higher toxicity compared to other materials, with cell viability reducing down to 75% after 24 h at a concentration of 2 mM. Increasing the FCA concentration to 20 mM elicited severe toxicity, resulting in a cellular viability below 70% (Fig. 3D). All the materials showed a concentration and time-dependent toxic behavior, except for PVA-SbQ and MWCNTs. The results suggest that these chemicals and NPs demonstrate minimal toxicity on the viability of the epidermal cells at an individual level, especially at the concentrations present in the sensor.

The keratinocytes treated with the chemical mixtures, Au_m, Ag_m, and $MWCNT_m$ were examined next. The data shows a cluster for the three mixtures for an exposure time of 2 h, indicating a similar cytotoxic nature (Fig. 3B). When exposure time is increased, the toxicity levels for the mixtures drift, with Ag_m exhibiting highest toxicity and $MWCNT_m$ exhibiting the lowest. Higher concentrations of Au_m and Ag_m showed acute toxic behavior (cell viability ~70%) similar to the individual NP treatment, but a greater loss in viability was elicited at lower concentrations compared to the individual NPs (Fig. 3E). The elevated toxicity levels can be attributed to the toxic nature of the FCA mediator present in the mixtures. It was noted that the $MWCNT_m$ also displayed slight toxicity at higher concentrations (< 85%) unlike at an individual level (Fig. 3B). The mixtures demonstrated higher toxicity (~10% increase) compared to the individual materials, which can be attributed to the combined effect of the individual materials. Regardless of the increase in the toxicity levels in mixtures, the toxicity was observed to be minimal at concentrations used in the wound monitoring sensor. To evaluate the biocompatibility of the biosensor itself, three different biosensors namely, Au_b, Ag_b and $MWCNT_b$ were examined. A cell viability of 79%, 77% and 87% was elicited after a 24 h treatment of the cells to the biosensor comprising of Au NPs, Ag NPs or MWCNTs respectively. These cell viabilities were higher (~3–5%) than that observed for the respective material mixtures. This improved cell viability can be attributed to the PVA-SbQ coating over the biosensor. The PVA-SbQ matrix acts as a biocompatible coating over the biosensor resulting in reduced leaching of the sensor materials, hence improving the cell viability.

To better visualize the kinetics behind the toxicity of these materials, time-lapse fluorescent microscopic images were captured to observe the cellular morphological changes over time (Supplementary Fig. S2). While the control illustrated a large number of viable cells with characteristic cuboidal geometries, the cells began to die after 2 h of treatment with Au and Ag NPs, as indicated by the increased number of rounded cells (Supplementary Fig. S2A and B). A considerable amount of live cells were observed after exposing the cells to UOx (Supplementary Fig. S2C) at lower concentrations. But the cells started dying on exposure to higher concentrations, as depicted by the rounded red-stained cells. The cells exposed to FCA also showed decreased viability, especially when treated for long periods of time. A change in the cell morphology was also induced from a well-defined cuboidal shape to a rounded shape (Supplementary Fig. S2D). However, the morphology of the cells subjected to MWCNTs and PVA-SbQ were comparable to the control cells (Supplementary Fig. S2E and F). The time-dependent fluorescence images for material mixtures were also captured in a similar manner. The wells with cells exposed to Au_m and Ag_m showed an increased number of dead cells at the concentrations present in the sensor, after a 24 h treatment (Fig. 3C). The cells exposed

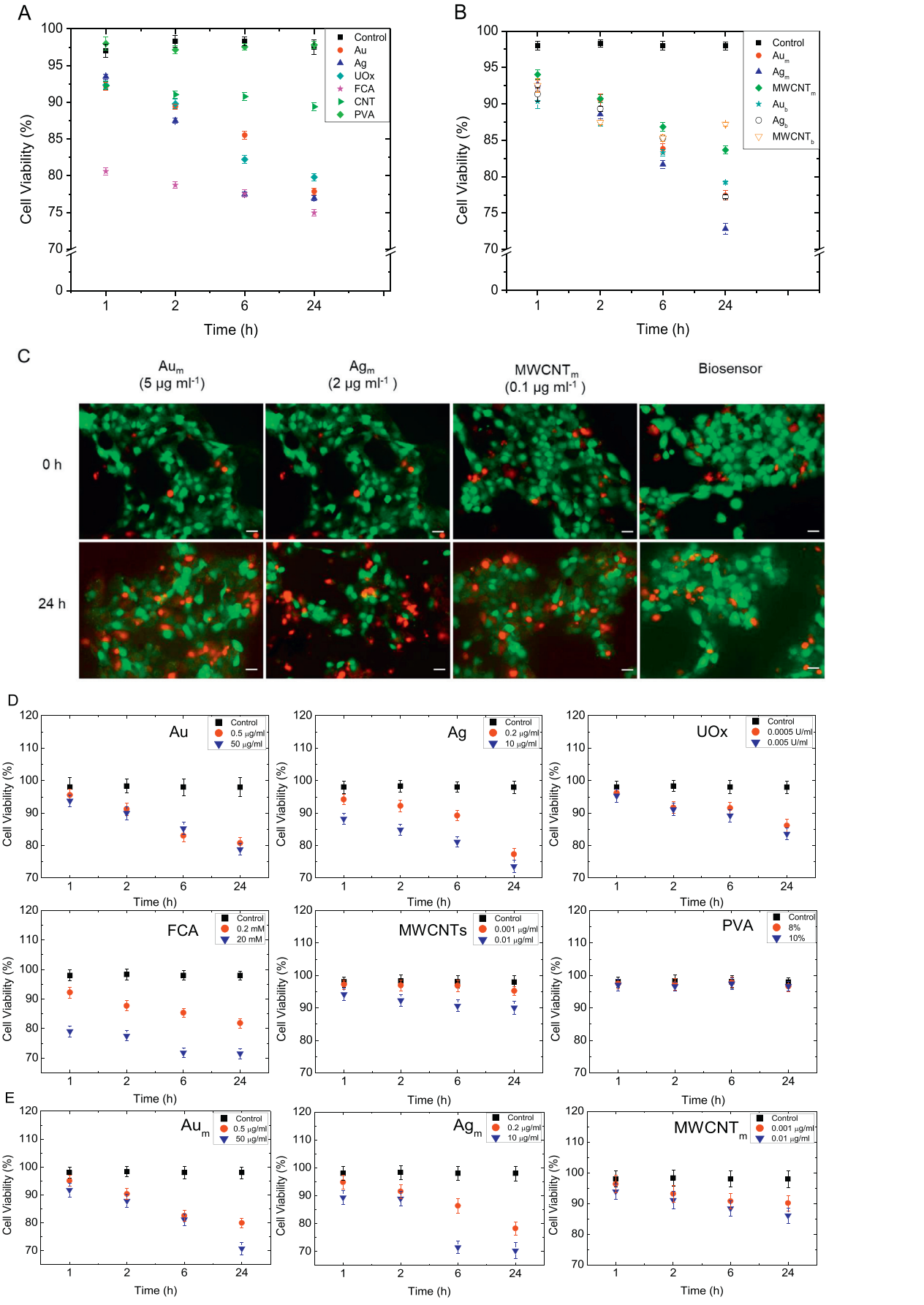

(caption on next page)

Fig. 3. Viability of cells after treating with the biosensor and its materials. (A) Au, Ag, UOx, FCA, MWCNTs and PVA-SbQ, (B) Au/UOx/FCA/PVA-SbQ (Au_m), Ag/UOx/FCA/PVA-SbQ (Ag_m), MWCNTs/UOx/FCA/PVA-SbQ ($MWCNT_m$) mixtures and the respective biosensors and (C) Live/Dead stained fluorescent images (20×) of cultured keratinocytes on exposure to Au_m, Ag_m, $MWCNT_m$ and the respective biosensors for 24 h. The control groups (0 h) indicate cells cultured only in growth media. (Scale bar: 20 μm). The green color illustrates the live cells while the red color represents the dead cells. (D) Au, Ag, UOx, FCA, MWCNT and PVA-SbQ and (E) Au/UOx/FCA/PVA-SbQ (Au_m), Ag/UOx/FCA/PVA-SbQ (Ag_m) and MWCNT/UOx/FCA/PVA-SbQ ($MWCNT_m$) mixtures at varying concentrations. (For interpretation of the references to color in this figure legend, the reader is referred to the web version of this article.)

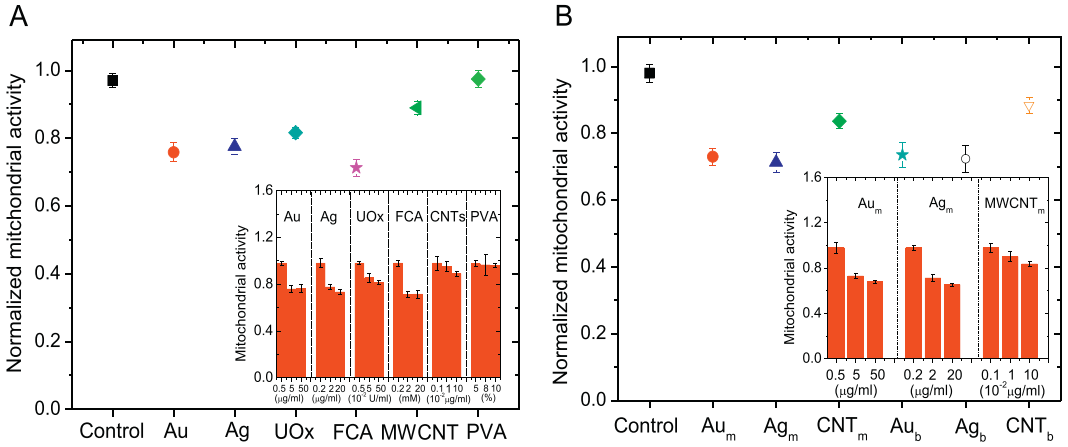

Fig. 4. Mitochondrial activity of cells after 24 h treatment with the biosensor and its materials. (A) Au, Ag, UOx, FCA, MWCNTs and PVA-SbQ and (B) Au/UOx/FCA/PVA-SbQ (Au_m), Ag/UOx/FCA/PVA-SbQ (Ag_m) and MWCNTs/UOx/FCA/PVA-SbQ ($MWCNT_m$) mixtures and the respective biosensors. The insets represent the mitochondrial activity of the cells on treatment with the materials and the respective mixtures at varying concentrations.

to the $MWCNT_m$ initially maintained a well-defined geometry, but some cells were observed to round up after 24 h (Fig. 3C). A similar trend was observed for the respective biosensors, with only a few cells exhibiting a rounded shape after a 24 h treatment, confirming its biocompatibility (Fig. 3C). It was evident from the time-lapse images that not many cells died on exposure to the materials or the biosensor, and the cell geometries were well-maintained at the concentrations present in the sensor for all the mixtures. The changes in the cellular morphology and the toxicity profiles depicted by the images below correlate well with the viability data.

3.2. Evaluation of mitochondrial activity

Fig. 4A shows the metabolic activity of the cells after being treated with individual materials at concentrations present in the sensor for 24 h. As seen in the figure, activity levels of MWCNTs and PVA-SbQ were above 0.85, suggesting no mitochondrial damage. The entire concentration range also showed no effect on the metabolic activity (Fig. 4A inset). In addition, the activity was seen to be time-independent with a normal activity being maintained even after an incubation time of 24 h. On the contrary, the NPs and the chemicals showed a slight decrease in the activity, implying reduced cellular metabolic rate (Fig. 4A). A further decrease in the activity levels was observed at higher concentrations of the NPs (Fig. 4A inset). The mitochondrial dysfunction caused by the NPs is known to have an inverse relationship with their size. Smaller NPs, of sizes ≤10 nm, result in the production of high superoxide levels, damaging mitochondrial function (Fu et al., 2014). The UOx enzyme also demonstrated a slight reduction in mitochondrial activity (~0.8), which may be due to the production of H_2O_2, as mentioned earlier (Fig. 4A). Previous studies have reported that H_2O_2 leads to reduction of NADPH levels inhibiting the mitochondrial respiration cycle (Nulton-Persson and Szweda, 2001). In case of FCA, a level of ~0.7 at concentrations above 0.2 mM is representative of impeded mitochondrial activity (Fig. 4A and Fig. 4A inset). All the assay results for the individual materials demonstrated minimal loss in the metabolic activity at concentrations present in the sensor; however, the mitochondrial activity was significantly lower at higher concentrations for both the NPs and the FCA mediator.

The mixtures, Au_m, Ag_m, $MWCNT_m$, and the biosensor were studied next for their effect on the cellular mitochondrial activity. Similar to the viability results, the combinations exhibited a higher reduction in activity compared to the individual materials, however, the differences were not as significant (SD ± 0.04). Stimulating the cells with both Au_m and Ag_m manifested a decrease in their metabolic activity (< 0.75) at the concentrations present in the sensor (Fig. 4B), and also showed a clear dose-response relationship (Fig. 4B inset). While the $MWCNT_m$ did not exhibit a very sharp decrease in the mitochondrial function (0.83), it was still higher than that observed for only MWCNTs (0.88) (Fig. 4B). The Au_b, Ag_b and $MWCNT_b$ were also seen to decrease the mitochondrial activity of the cells. However, the metabolic activity for all the biosensors was recorded to be lower than the mixtures, which can be attributed to the reduced leaching of the sensor materials due to the protective layer offered by the PVA-SbQ matrix. Although the resazurin assay provides a good overview of the overall effect on mitochondrial activity, direct assays like measurement of ROS and mitochondrial membrane potential can be employed in the future studies to gain better insight about the induced mitochondrial damage.

3.3. Evaluation of cellular apoptosis

The percentage of apoptotic cells after exposure to the individual materials after 24 h was recorded as shown in Fig. 5A. While Au NPs, MWCNTs and PVA-SbQ expressed no apoptotic cells, around 5% of the cells expressed apoptotic activity when exposed to Ag NPs. A lesser number of apoptotic cells were expressed on exposure to FCA and the UOx enzyme (~3.5%) at the concentrations present in the sensor. The results further indicated that Ag NPs had a higher apoptosis inducing ability compared to the Au NPs. A concentration of only 2 μg ml^{-1} of Ag NPs has a higher apoptotic activity (4.89%) compared to that of 50 μg ml^{-1} of Au NPs (3.1%) (Fig. 5A and Fig. 5A inset). The slight apoptotic activity demonstrated by the UOx enzyme may again be induced as a result of the H_2O_2 production (Fig. 5A). In the case of FCA, an increase in the concentration notably up-regulated the number of apoptotic cells, confirming that this compound induces cell death via the intrinsic pathway at higher concentrations (Fig. 5A inset).

The apoptosis, as induced by the respective mixtures and the

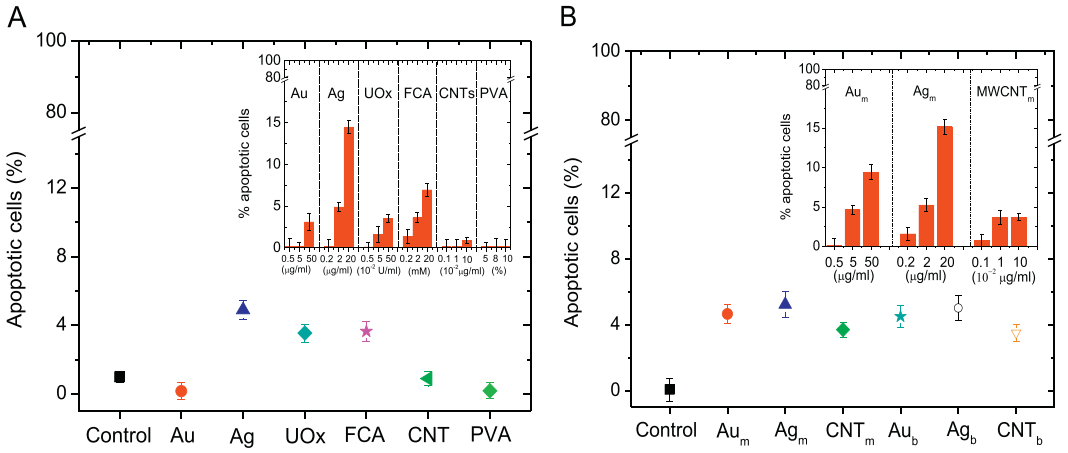

Fig. 5. Apoptotic activity of cells after 24 h treatment with the biosensor and its materials. (A) Au, Ag, UOx, FCA, MWCNTs and PVA-SbQ and (B) Au/UOx/FCA/PVA-SbQ (Au_m), Ag/UOx/FCA/PVA-SbQ (Ag_m), MWCNT/UOx/FCA/PVA-SbQ ($MWCNT_m$) mixtures and the respective biosensors. The insets represent the apoptotic activity of the cells on treatment with the materials and the respective mixtures at varying concentrations.

biosensors, is illustrated in Fig. 5B. As depicted in the figure, all the mixtures and the biosensors demonstrated a similar level of caspase-3/7 activity induction. The Ag_m exhibited the highest percentage (5.23%) of apoptotic cells due to the presence of both Ag and FCA in the mixture. The Ag_m had higher activity levels in comparison to Au_m (4.65%) and $MWCNT_m$ (3.7%). The apoptotic activity induced by these mixtures was higher than the NP treatments alone, with an increase in the number of apoptotic cells expressed by about 3%. This can be explained by the apoptotic nature of the FCA and UOx present in the mixture. It was further seen that increasing the concentrations of all the materials caused an increase in the caspase activity, with Ag_m expressing around 15% apoptotic cells at higher concentrations (Fig. 5B inset). Thereafter, the apoptotic activity of the cells after treatment to the biosensor itself was investigated. The percentage of expressed apoptotic cells was observed to be 4.5%, 5.02% and 3.5% for Au_b, Ag_b and $MWCNT_b$ respectively, which was lower than the respective mixtures. The decreased apoptosis by the biosensor may again be attributed to the reduced percolation of the sensor materials through the PVA-SbQ matrix. The obtained data confirms that none of the mixtures or the biosensors induce any prononuced apoptotic activity even at higher concentrations.

4. Conclusion

In this work, six different materials used in a wound monitoring sensor were investigated for their cytotoxicity, both individually and as mixtures on human keratinocytes. The time-lapse studies indicated that the materials in the sensor show minimal toxicity at the concentrations present in the sensor. The cells were seen to undergo a morphological change from a cuboidal geometry (live) to a spherical geometry (dead) when exposed to the materials. Resazurin assay confirmed no considerable impairment of the mitochondrial function at low concentrations of the materials. An apoptotic assessment assay was also carried out wherein Ag NPs and FCA mediator exhibited a slight apoptotic behavior compared to the other sensor materials. It was established from these assays that the materials and the respective mixtures incur only a minimal loss in viability, mitochondrial damage, and apoptosis on exposure at concentrations present in the sensors. Further, the toxicity assays were carried out at a sensor level to establish the biocompatibility of the biosensor itself. It was observed that the biosensor exhibited lower toxicity levels compared to the sensor material mixtures. This improved biocompatibility was attributed to the biocompatible protective layer offered by the PVA-SbQ matrix resulting in reduced leaching of the sensor materials. To fully examine and understand the underlying toxicity mechanisms, more specific and direct studies will need to be carried out in the future. The studies confirm the biocompatibility of the reported sensor and show that it can be used for continuous wound monitoring applications. However, the electron mediator FCA was seen to be highly toxic at higher concentrations; hence, mediator-based sensors should be carefully evaluated for wound monitoring applications.

Acknowledgment

This work is being supported by the NSF Nanosystems Engineering Research Centre for Advanced Self-Powered Systems of Integrated Biosensors and Technologies (ASSIST) under Award Number (EEC-1160483).

Conflict of interest

The authors declare no conflict of interest.

Appendix A. Supplementary data

Supplementary data to this article can be found online at https://doi.org/10.1016/j.tiv.2019.03.034.

References

Alarifi, S., Ali, D., Verma, A., Alakhtani, S., Ali, B.A., 2013. Cytotoxicity and genotoxicity of copper oxide nanoparticles in human skin keratinocytes cells. Int. J. Toxicol. 32, 296–307.

Arora, S., Jain, J., Rajwade, J., Paknikar, K., 2008. Cellular responses induced by silver nanoparticles: in vitro studies. Toxicol. Lett. 179, 93–100.

Bastos, V., de Oliveira, J.F., Brown, D., Jonhston, H., Malheiro, E., Daniel-da-Silva, A., Duarte, I., Santos, C., Oliveira, H., 2016. The influence of citrate or PEG coating on silver nanoparticle toxicity to a human keratinocyte cell line. Toxicol. Lett. 249, 29–41.

Burd, A., Kwok, C.H., Hung, S.C., Chan, H.S., Gu, H., Lam, W.K., Huang, L., 2007. A comparative study of the cytotoxicity of silver-based dressings in monolayer cell, tissue explant, and animal models. Wound Repair Regen. 15, 94–104.

Carrola, J., Bastos, V., Jarak, I., Oliveira-Silva, R., Malheiro, E., Daniel-da-Silva, A.L., Oliveira, H., Santos, C., Gil, A.M., Duarte, I.F., 2016. Metabolomics of silver nanoparticles toxicity in HaCaT cells: structure–activity relationships and role of ionic silver and oxidative stress. Nanotoxicology 10, 1105–1117.

Ding, L., Stilwell, J., Zhang, T., Elboudwarej, O., Jiang, H., Selegue, J.P., Cooke, P.A., Gray, J.W., Chen, F.F., 2005. Molecular characterization of the cytotoxic mechanism of multiwall carbon nanotubes and nano-onions on human skin fibroblast. Nano Lett. 5, 2448–2464.

Fu, P.P., Xia, Q., Hwang, H.-M., Ray, P.C., Yu, H., 2014. Mechanisms of nanotoxicity: generation of reactive oxygen species. J. Food Drug Anal. 22, 64–75.

Galandáková, A., Frankova, J., Ambrožová, N., Habartova, K., Pivodova, V., Zálešák, B., Šafářová, K., Smekalova, M., Ulrichova, J., 2016. Effects of silver nanoparticles on human dermal fibroblasts and epidermal keratinocytes. Hum. Exp. Toxicol. 35, 946–957.

Goodman, C.M., McCusker, C.D., Yilmaz, T., Rotello, V.M., 2004. Toxicity of gold nanoparticles functionalized with cationic and anionic side chains. Bioconjug. Chem. 15, 897–900.
Grudzinski, I.P., Bystrzejewski, M., Cywinska, M.A., Kosmider, A., Poplawska, M., Cieszanowski, A., Ostrowska, A., 2013. Cytotoxicity evaluation of carbon-encapsulated iron nanoparticles in melanoma cells and dermal fibroblasts. J. Nanopart. Res. 15, 1835.
Holmes, A.M., Lim, J., Studier, H., Roberts, M.S., 2016. Varying the morphology of silver nanoparticles results in differential toxicity against micro-organisms, HaCaT keratinocytes and affects skin deposition. Nanotoxicology 10, 1503–1514.
Huang, C.-Y., Hu, K.-H., Wei, Z.-H., 2016. Comparison of cell behavior on pva/pva-gelatin electrospun nanofibers with random and aligned configuration. Sci. Rep. 6, 37960.
Kyung, O.Y., Grabinski, C.M., Schrand, A.M., Murdock, R.C., Wang, W., Gu, B., Schlager, J.J., Hussain, S.M., 2009. Toxicity of amorphous silica nanoparticles in mouse keratinocytes. J. Nanopart. Res. 11, 15–24.
Monteiro-Riviere, N.A., Nemanich, R.J., Inman, A.O., Wang, Y.Y., Riviere, J.E., 2005. Multi-walled carbon nanotube interactions with human epidermal keratinocytes. Toxicol. Lett. 155, 377–384.
Nulton-Persson, A.C., Szweda, L.I., 2001. Modulation of mitochondrial function by hydrogen peroxide. J. Biol. Chem. 276, 23357–23361.
Poon, V.K., Burd, A., 2004. In vitro cytotoxity of silver: implication for clinical wound care. Burns 30, 140–147.
RoyChoudhury, S., Umasankar, Y., Bhansali, S., 2017. A wearable electrochemical sensor to monitor progression of wound healing. ECS Trans. 80, 1345–1353.
RoyChoudhury, S., Umasankar, Y., Hutcheson, J.D., Lev-Tov, H.A., Kirsner, R.S., Bhansali, S., 2018. Uricase Based Enzymatic Biosensor for Non-Invasive Detection of Uric Acid by Entrapment in PVA-SbQ Polymer Matrix. Electroanalysis 30, 2374–2385.
Schaeublin, N.M., Braydich-Stolle, L.K., Schrand, A.M., Miller, J.M., Hutchison, J., Schlager, J.J., Hussain, S.M., 2011. Surface charge of gold nanoparticles mediates mechanism of toxicity. Nanoscale 3, 410–420.
Shang, L., Nienhaus, K., Nienhaus, G.U., 2014. Engineered nanoparticles interacting with cells: size matters. J. Nanobiotechnol. 12, 5.
Shukla, R.K., Kumar, A., Pandey, A.K., Singh, S.S., Dhawan, A., 2011. Titanium dioxide nanoparticles induce oxidative stress-mediated apoptosis in human keratinocyte cells. J. Biomed. Nanotechnol. 7, 100–101.
Shvedova, A., Castranova, V., Kisin, E., Schwegler-Berry, D., Murray, A., Gandelsman, V., Maynard, A., Baron, P., 2003. Exposure to carbon nanotube material: assessment of nanotube cytotoxicity using human keratinocyte cells. J. Toxicol. Environ. Health Part A 66, 1909–1926.
Swain, S.K., Sarkar, D., 2014. Fabrication, bioactivity, in vitro cytotoxicity and cell viability of cryo-treated nanohydroxyapatite–gelatin–polyvinyl alcohol macroporous scaffold. J. Asian Ceram. Soc. 2, 241–247.
Thang, P.T., Teik, L.S., Yung, C.S., 2001. Anti-oxidant effects of the extracts from the leaves of Chromolaena odorata on human dermal fibroblasts and epidermal keratinocytes against hydrogen peroxide and hypoxanthine–xanthine oxidase induced damage. Burns 27, 319–327.
Tian, F., Cui, D., Schwarz, H., Estrada, G.G., Kobayashi, H., 2006. Cytotoxicity of single-wall carbon nanotubes on human fibroblasts. Toxicol. in Vitro 20, 1202–1212.